

Shielding Failure Current of Overhead Transmission Lines Generated through an ATPDraw Object

Z. G. Datsios, P. N. Mikropoulos, T. E. Tsovilis

Abstract—The maximum shielding failure current of overhead transmission lines is an important parameter in evaluating the shielding performance of the lines and performing insulation coordination studies of the connected substations. A new ATPDraw object has been developed, by using MODELS language, that easily generates the maximum shielding failure current of overhead transmission lines, with amplitude and waveshape depending on line geometry and selected lightning attachment model. The new object, called MSFC, was employed in ATP-EMTP simulations of a 150 kV GIS substation. The computed shielding failure surges impinging on the substation, being dependent upon maximum shielding failure current, vary considerably among lightning attachment models. The MSFC object is a useful tool within the ATP-EMTP environment in assessing the shielding failure surges arising at overhead transmission lines and impinging on the connected substations.

Keywords: ATP-EMTP, ATPDraw, GIS substation, insulation coordination, lightning surges, maximum shielding failure current, MODELS, overhead transmission lines.

I. INTRODUCTION

SHIELDING failure of overhead transmission lines, that is direct lightning strokes to phase conductors, is one of the main causes of line outages and may also result in substation outages, caused by incoming surges with amplitude exceeding the insulation level of substation equipment. Shielding of overhead transmission lines against direct lightning strokes to phase conductors is provided by shield wires, which intercept the descending lightning leader through a connecting upward discharge. However, some of the less intense strokes may not be intercepted and strike to phase conductors. Hence, there is a range of currents of lightning strokes that may terminate to phase conductors. The upper limit of this range, called maximum shielding failure current, can be estimated with the aid of general expressions derived by employing several lightning attachment models in shielding analysis [1]. The maximum shielding failure current of overhead transmission lines is an important parameter for insulation coordination studies; it greatly determines the shielding performance of the lines and is the upper limit of all possible shielding failure currents impinging on the connected substations.

Z. G. Datsios, P. N. Mikropoulos and T. E. Tsovilis are with the High Voltage Laboratory, Department of Electrical Energy, School of Electrical and Computer Engineering, Faculty of Engineering, Aristotle University of Thessaloniki, Thessaloniki 54124 Greece. (e-mail: zdatsios@auth.gr, pnm@eng.auth.gr, tsovilis@ee.auth.gr).

Paper submitted to the International Conference on Power Systems Transients (IPST2011) in Delft, the Netherlands June 14-17, 2011

In the present study a new ATPDraw [2] object has been developed by using MODELS language [3], [4], with the aid of which the maximum shielding failure current of overhead transmission lines is generated, with an amplitude depending on line geometry and selected lightning attachment model and waveshape in accordance with CIGRE [5]. The new object, called MSFC, has been applied to a typical 150 kV line of the Hellenic transmission system on the basis of several lightning attachment models; there is a great variability in maximum shielding failure current, in terms of both amplitude and waveshape, among lightning attachment models. Furthermore, the MSFC object was employed in ATP-EMTP [6] simulations to demonstrate the dependence of the computed overvoltages impinging on a 150 kV GIS substation upon maximum shielding failure current of the connected transmission lines. The computed overvoltages vary significantly among lightning attachment models used in simulations; this variation has been easily quantified with the aid of the new ATPDraw object.

II. MAXIMUM SHIELDING FAILURE CURRENT OF OVERHEAD TRANSMISSION LINES

A. Amplitude

Based on shielding analysis of overhead transmission lines, as detailed in a previous study [1], the maximum shielding failure current amplitude, I_{MSF} (kA), can be calculated according to different categories of lightning attachment models by using the following general expressions

Electrogeometric models [7]-[17]

$$I_{MSF} = \left[\frac{\gamma(h_m + h_p)/2}{A(1 - \gamma \sin \alpha)} \right]^{\frac{1}{B}} \quad (1)$$

A. J. Eriksson's model [18]

$$I_{MSF} = \left[\frac{\Delta R + \sqrt{\Delta R^2 + \Psi^2(\Gamma^2 - 1)}}{0.67 h_p^{0.6} (\Gamma^2 - 1)} \right]^{0.74} \quad (2)$$

$$\Delta R = (h_m - h_p) \tan \alpha, \quad \Gamma = (h_m/h_p)^{0.6}, \quad \Psi^2 = (h_m - h_p)^2 + \Delta R^2$$

Generic models [19]-[24]

$$I_{MSF} = \left[\frac{(h_m - h_p) \tan \alpha - \zeta(h_m^G - h_p^G)}{\xi(h_m^E - h_p^E)} \right]^{\frac{1}{F}} \quad (3)$$

Statistical model [25]-[27]

$$I_{MSF} = \left[\frac{(h_m - h_p) \tan \alpha + 0.01 h_m^{1.3}}{2.72 \ln(h_m/h_p)} \right]^{\frac{1}{0.65}} \quad (4)$$

where factors A, B, γ are given in Table I; factors ξ, E, F, ζ, G are given in Table II; h_m (m), h_p (m), are the height of the shield wire and phase conductor, respectively, and α is the shielding angle.

TABLE I
FACTORS A, B AND γ TO BE USED IN (1)

Electrogeometric model	A	B	γ
Wagner & Hileman [7]	14.2	0.42	1
Young et al. [8]	27γ	0.32	$1 \text{ for } h_m < 18 \text{ m}$ $\frac{444}{462-h_m} \text{ for } h_m > 18 \text{ m}$
Armstrong & Whitehead [9]	6.72	0.80	1.11
Brown & Whitehead [10]	7.1	0.75	1.11
Love [11]	10	0.65	1
Whitehead [12]	9.4	0.67	1
Suzuki et al. [13] from Golde [14]	3.3	0.78	1
Anderson [15], IEEE WG [16]	8	0.65	$1/\beta^i$
IEEE Std [17]	10	0.65	$1/\beta^{ii}$

ⁱ $\beta = 0.64$ for UHV lines, 0.8 for EHV lines and 1 for other lines
ⁱⁱ $\beta = 0.36 + 0.17 \ln(43-h_p)$ for $h_p < 40$ m, $\beta = 0.55$ for $h_p > 40$ m

TABLE II
FACTORS ξ, E, F, ζ AND G TO BE USED IN (3)

Generic model	ξ	E	F	ζ	G
Rizk [19]	1.57	0.45	0.69	0	0
Petrov et al. [20] ⁱ	0.47	0.67	0.67	0	0
Borghetti et al. [21] from Dellera & Garbagnati [22]	0.028	1	1	3	0.6
Ait-Amar & Berger [23]	3	0.20	0.67	0	0
Cooray & Becerra [24]	2.17	0.5	0.57^{ii}	0	0

ⁱ using as h in (3) the object height plus 15 m

ⁱⁱ average value adapted from [24] for conductor height up to 50 m

B. Waveshape

The shielding failure current waveshape is generated based on the lightning current expressions proposed by CIGRE [5]. The upwardly concave wavefront, expressed by (5), lasts up to the 90% of the amplitude where the maximum steepness is observed; this corresponds to the instant t_n (μs), given by (6).

$$I = A_1 t + B_1 t^n \quad (5)$$

$$t_n = 0.6 t_f \left[3 S_N^2 / (1 + S_N^2) \right] \quad (6)$$

In (5) and (6) I (kA) is the instantaneous lightning current, t (μs) is the time instant, n , A_1 (kA/μs), B_1 (kA/μsⁿ) and S_N are constants given by (7), (8), (9) and (10), respectively, and t_f (μs) is the front time.

$$n = 1 + 2(S_N - 1)(2 + 1/S_N) \quad (7)$$

$$A_1 = [1/(n-1)] [(0.9n \cdot I_{MSF}/t_n) - S_m] \quad (8)$$

$$B_1 = [1/(t_n^n(n-1))] (S_m t_n - 0.9 I_{MSF}) \quad (9)$$

$$S_N = S_m t_f / I_{MSF} \quad (10)$$

In (7)-(10) I_{MSF} (kA) is the maximum shielding failure current amplitude and S_m (kA/μs) is the maximum steepness. The shielding failure current wavetail is given as

$$I = I_1 \exp[-(t - t_n)/t_1] - I_2 \exp[-(t - t_n)/t_2] \quad (11)$$

where I_1 (kA), I_2 (kA), t_1 (μs) and t_2 (μs) are constants expressed by (12), (13), (14) and (15), respectively, t_h (μs) is the time to half value.

$$I_1 = [(t_1 \cdot t_2) / (t_1 - t_2)] (S_m + 0.9 I_{MSF} / t_2) \quad (12)$$

$$I_2 = [(t_1 \cdot t_2) / (t_1 - t_2)] (S_m + 0.9 I_{MSF} / t_1) \quad (13)$$

$$t_1 = (t_h - t_n) / \ln 2 \quad (14)$$

$$t_2 = 0.1 I_{MSF} / S_m \quad (15)$$

The median values of the front time, t_f (μs), and maximum steepness, S_m (kA/μs), are given by (16) and (17), respectively, and the time to half value is taken as 77.5 μs [5].

$$t_f = \begin{cases} 1.77 I_{MSF}^{0.188}, & 3 \leq I_{MSF} \leq 20 \text{ kA} \\ 0.906 I_{MSF}^{0.411}, & I_{MSF} > 20 \text{ kA} \end{cases} \quad (16)$$

$$S_m = \begin{cases} 12 I_{MSF}^{0.171}, & 3 \leq I_{MSF} \leq 20 \text{ kA} \\ 6.5 I_{MSF}^{0.376}, & I_{MSF} > 20 \text{ kA} \end{cases} \quad (17)$$

III. MSFC OBJECT

The new ATPDraw [2] object, called MSFC, generates the maximum shielding failure current of overhead transmission lines based on the analysis detailed above. The MSFC object has been developed by using MODELS language [3], [4] and incorporates a MODEL that controls a TACS Type 60 current source.

Fig. 1 shows the ATPDraw dialog box of the MSFC object; the user enters the input data, namely the height of the shield wire, h_m (m), the height of the phase conductor, h_p (m), and the shielding angle (deg) of the overhead transmission line. The user also selects the lightning attachment model to be used in calculations, by assigning a value to the parameter model selection (MS), ranging from 1 to 16 corresponding to the adopted lightning attachment model numbered in Table III.

Hence, with the aid of the MSFC object the maximum shielding failure current of overhead transmission lines is easily generated in the ATP-EMTP environment. Fig. 2 shows the maximum shielding failure current of the upper phase conductor of a typical 150 kV line of the Hellenic transmission system (Fig. 3), generated by the MSFC object based on several lightning attachment models. Table III summarizes the basic characteristics of the maximum shielding failure current of the 150 kV line obtained by the MSFC object.

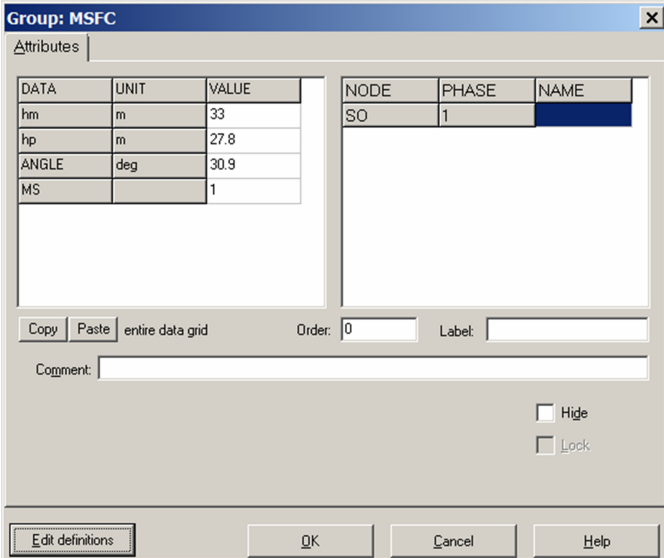


Fig. 1. ATPDraw input dialog box of the developed MSFC object.

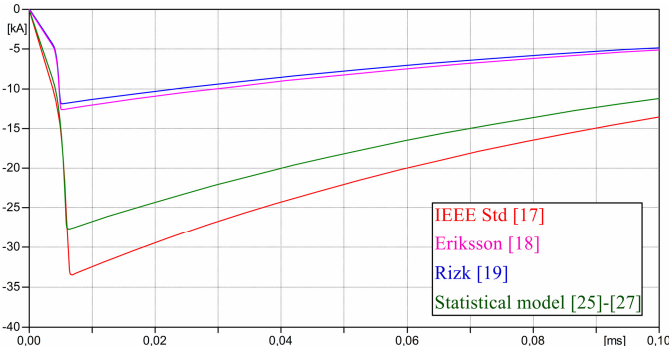


Fig. 2. Maximum shielding failure current of the upper phase conductor of a typical 150 kV overhead line of the Hellenic transmission system.

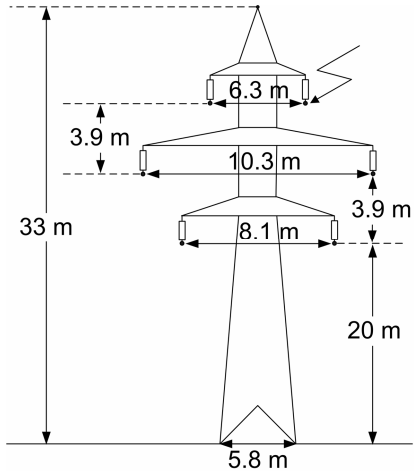


Fig. 3. Tower of a typical 150 kV double circuit overhead line of the Hellenic transmission system and lightning stroke location considered in simulations; shielding angle of the upper phase conductor 30.9°.

From both Fig. 2 and Table III it is obvious that there is a great variability in maximum shielding failure current, in terms of both amplitude and waveshape, among lightning attachment models. This may affect significantly the computed shielding failure surges arising at the overhead transmission lines, thus also impinging on the connected substations. The latter is demonstrated in what follows.

TABLE III

MAXIMUM SHIELDING FAILURE CURRENT OF THE UPPER PHASE CONDUCTOR OF THE 150 kV OVERHEAD TRANSMISSION LINE

No	Lightning attachment model	I_{MSF} (kA)	t_f (μs)	S_m (kA/μs)
1	Wagner & Hileman [7]	34.0	3.86	24.48
2	Young et al. [8]	15.5	2.96	19.17
3	Armstrong & Whitehead [9]	21.7	3.21	20.67
4	Brown & Whitehead [10]	24.7	3.38	21.71
5	Love [11]	16.8	3.01	19.44
6	Whitehead [12]	16.9	3.01	19.46
7	Suzuki et al. [13] from Golde [14]	43.4	4.27	26.83
8	Anderson [15], IEEE WG [16]	23.6	3.32	21.34
9	IEEE Std [17]	33.6	3.84	24.37
10	Eriksson [18]	12.7	2.85	18.53
11	Rizk [19]	11.9	2.82	18.33
12	Petrov et al. [20]	17.1	3.02	19.50
13	Borghetti et al. [21] from Delleria & Garbagnati [22]	5.0	2.40	15.80
14	Ait-Amar & Berger [23]	58.6	4.83	30.04
15	Cooray & Becerra [24]	7.0	2.55	16.74
16	Statistical model [25]-[27]	27.7	3.55	22.66

IV. APPLICATION OF THE MSFC OBJECT FOR THE EVALUATION OF SHIELDING FAILURE SURGES IMPINGING ON SUBSTATIONS

Substation outages may be caused by impinging overvoltage surges, due to backflashover or shielding failure of the incoming overhead transmission lines, exceeding the insulation level of substation equipment. The MSFC object was employed in ATP-EMTP [6] simulations for the evaluation of the overvoltage surges impinging on a 150 kV GIS substation due to shielding failure of the incoming overhead transmission lines; the overvoltage surges due to backflashover impinging on the same substation were computed before [28]. The tower geometry of a typical 150 kV double circuit overhead line of the Hellenic transmission system and the configuration of the evaluated substation are shown in Figs. 3 and 4, respectively.

Simulations were performed for the following worst case scenario: negative lightning is assumed to strike the upper phase conductor of the double circuit transmission line, at the first tower close to the substation, at the time instant of negative power-frequency voltage peak. The lightning current is generated by the MSFC object with basic characteristics as shown in Table III. The last section of the incoming overhead transmission line, 1.75 km in length, was represented by a sequence of J.Marti frequency-dependent models, considering the line span (350 m) and the tower geometry shown in Fig. 3. Towers were represented as vertical lossless single-phase frequency-independent distributed parameter lines with a surge impedance of 167 Ω, calculated according to [16], [29]. Towers were terminated by a constant grounding resistance of 10 Ω [30]. Line insulator strings, with standard lightning impulse withstand voltage level of 750 kV and length of 1.86 m, were represented by voltage-dependent flashover switches

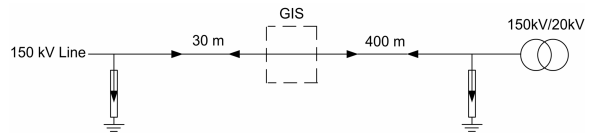


Fig. 4. Schematic diagram of the evaluated 150 kV GIS substation.

controlled by a MODEL implementing Weck's leader development model [5], [31]. The underground XLPE power cables were represented by the Bergeron model with parameters calculated at 500 kHz. Surge arresters were represented by the Pinceti and Giannettoni frequency-dependent model [32] as shown in Fig. 5, with parameters calculated based on the surge arrester characteristics given in Table IV. GIS bays were represented as lossless stub lines with a surge impedance of 75Ω [31]. The step-up transformer was represented by a capacitance pi-circuit together with a BCTRAN model. Cable connections and surge arrester lead lengths shorter than 3 m were modeled by a lumped parameter inductance of $1 \mu\text{H}/\text{m}$ [31]. The earth resistivity was assumed $200 \Omega\text{m}$. Finally, simulations were performed with and without surge arresters operating at the line-cable junction so as to evaluate the protection offered against impinging surges with respect to the basic insulation level, BIL, of the GIS system (750 kV), considering also a safety factor of 1.15 [33].

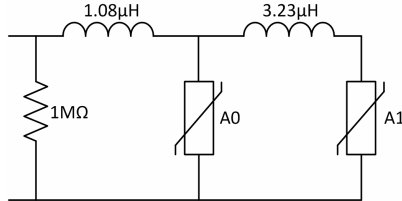


Fig. 5. Frequency-dependent surge arrester model [32]; parameters calculated based on the surge arrester characteristics given in Table IV.

TABLE IV
SURGE ARRESTER CHARACTERISTICS

System voltage	Rated voltage	Residual voltage 10 kA, 8/20 μs	Residual voltage 10 kA, 1/2 μs
150 kV	144 kV	346 kV	377 kV

Fig. 6(a) shows the computed overvoltages arising at the 150 kV GIS entrance, associated with maximum shielding failure currents generated by the MSFC object for several lightning attachment models, without surge arresters operating at the line-cable junction. The computed overvoltage, being dependent upon maximum shielding failure current, varies notably in terms of both peak and waveshape, among the lightning attachment models implemented in the MSFC object. However, it is obvious from Fig. 6(b) that this is less pronounced when surge arresters are operating at the line-cable junction according to common practice [34].

Fig. 7 summarizes the computed peak overvoltages arising at the 150 kV GIS entrance, obtained by using the maximum shielding failure current generated by the MSFC object with basic characteristics as shown in Table III. It is obvious that when surge arresters are not operating at the line-cable junction, the peak overvoltage varies significantly within the range of about 50% to 175% of the BIL among lightning attachment models. This is not the case when surge arresters are installed at the line-cable junction; the computed peak overvoltage varies lesser taking values significantly lower than the BIL (<65%) of the 150 kV GIS system. In addition, the peak overvoltage computed by selecting the generic

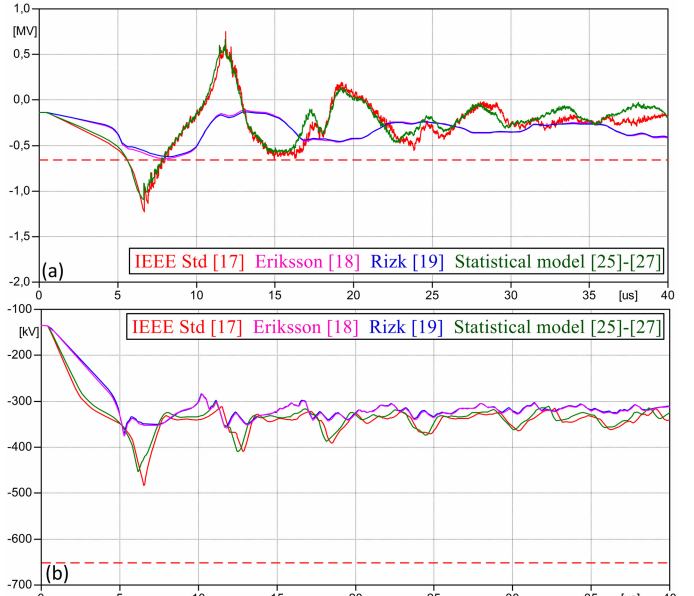


Fig. 6. Overvoltage at the entrance of the 150 kV GIS substation due to shielding failure of the incoming line; dashed line depicts the safety margin of BIL/1.15, (a) and (b) without and with surge arresters operating at the line-cable junction, respectively.

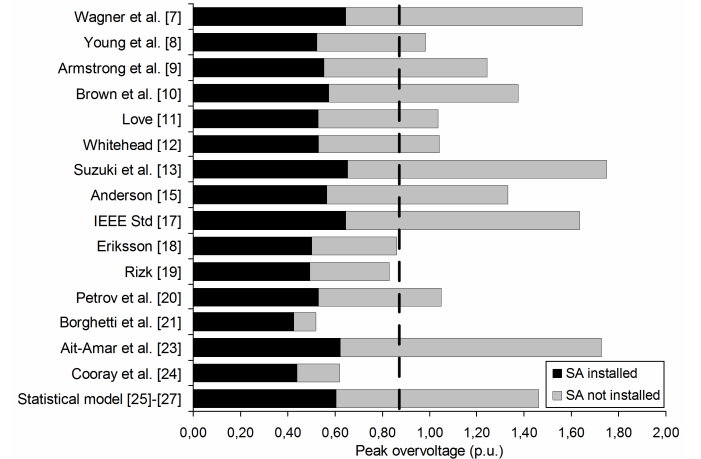


Fig. 7. Peak overvoltages arising at the entrance of the 150 kV GIS substation due to shielding failure of the incoming line, with and without surge arresters operating at the line-cable junction; 1 p.u. = 750 kV, dashed line depicts the safety margin of BIL/1.15.

models [19], [21] and [24] in MSFC object, contrary to that obtained from the rest lightning attachment models, do not indicate the need for surge arresters operating at the line-cable junction. It must be noted that the 150 kV GIS is connected to an overhead line through an underground cable (Fig. 4) and for such a configuration IEC [33] generally suggests the installation of surge arresters at the line-cable junction.

Finally, in the present study, the MSFC object was used in ATP-EMTP to compute the shielding failure surges impinging on the entrance of a GIS substation. It is well known that depending on substation layout, higher overvoltages may arise at other locations within GIS or along cables. These overvoltages would also be affected by lightning attachment models and this effect can be easily quantified with the aid of the MSFC object.

V. CONCLUSIONS

A new ATPDraw object, called MSFC, has been developed by using MODELS language. The MSFC object easily generates the maximum shielding failure current of overhead transmission lines, with amplitude and waveshape depending on line geometry and selected lightning attachment model.

The MSFC object was employed in ATP-EMTP simulations of a 150 kV GIS substation. The computed shielding failure surges impinging on the substation, being dependent upon maximum shielding failure current, vary significantly in terms of both amplitude and waveshape among the selected lightning attachment models; such variation may affect the selection of the required protection measures and standard insulation level of the substation equipment.

The MSFC object is a useful tool within the ATP-EMTP environment for utilities in assessing the shielding failure surges arising at overhead transmission lines and impinging on the connected substations, as well as in selecting the necessary protection measures. The MSFC object can also be used for educational purposes in high voltage engineering courses and it is available at <http://www.eng.auth.gr/hvl/>.

VI. REFERENCES

- [1] P. N. Mikropoulos and T. E. Tsovilis, "Lightning attachment models and maximum shielding failure current of overhead transmission lines: Implications in insulation coordination of substations," *IET Gener. Transm. Distrib.*, vol. 4, no. 12, pp. 1299-1313, Dec. 2010.
- [2] L. Prikler and H. K. Høidalen, "ATPDRAW version 3.5 Users' Manual," SINTEF Energy Research, Norway, 2002.
- [3] L. Dubé, "MODELS in ATP, language manual," Feb. 1996.
- [4] L. Dubé, "Users' guide to MODELS in ATP," Apr. 1996.
- [5] CIGRE Working Group 33.01, "Guide to procedures for estimating the lightning performance of transmission lines," *Technical Bulletin 63*, Oct. 1991.
- [6] Canadian-American EMTP Users Group, "ATP Rule Book," 1997.
- [7] C. F. Wagner and A. R. Hileman, "The lightning stroke-II," *AIEE Trans. PA&S*, vol. 80, no. 3, pp. 622-642, Apr. 1961.
- [8] F. S. Young, J. M. Clayton, and A. R. Hileman, "Shielding of transmission lines," *IEEE Trans. Power App. Syst.*, vol. PAS-82, no. 4, pp. 132-154, 1963.
- [9] H. R. Armstrong and E. R. Whitehead, "Field and analytical studies of transmission line shielding," *IEEE Trans. Power App. Syst.*, vol. PAS-87, no. 1, pp. 270-281, Jan. 1968.
- [10] G. W. Brown and E. R. Whitehead, "Field and analytical studies of transmission line shielding-II," *IEEE Trans. Power App. Syst.*, vol. PAS-88, no. 5, pp. 617-626, May 1969.
- [11] E. R. Love, "Improvements in lightning stroke modeling and applications to design of EHV and UHV transmission lines," M.Sc. thesis, Univ. Colorado, Denver, CO, 1973.
- [12] E. R. Whitehead, "CIGRE survey of the lightning performance of EHV transmission lines," *Electra*, no. 33, pp. 63-89, Mar. 1974.
- [13] T. Suzuki, K. Miyake, and T. Shindo, "Discharge path model in model test of lightning strokes to tall mast," *IEEE Trans. Power App. Syst.*, vol. PAS-100, no. 7, pp. 3553-3562, Jul. 1981.
- [14] R. H. Golde, "The frequency of occurrence and the distribution of lightning flashes to transmission lines," *AIEE Trans.*, vol. 64, no. 12, pp. 902-910, Dec. 1945.
- [15] J. G. Anderson, *Transmission Line Reference Book - 345 kV and above*, 2nd ed. Palo Alto, CA: Electric Power Research Institute, 1982, ch. 12.
- [16] IEEE Working Group, "A Simplified method for estimating lightning performance of transmission lines," *IEEE Trans. Power App. Syst.*, vol. PAS-104, no. 4, pp. 919-932, Jul. 1985.
- [17] *IEEE Guide for improving the Lightning performance of Transmission Lines*, IEEE Std. 1243-1997, Dec. 1997.
- [18] A. J. Eriksson, "An improved electrogeometric model for transmission line shielding analysis," *IEEE Trans. Power Del.*, vol. 2, no. 3, pp. 871-886, Jul. 1987.
- [19] F. A. M. Rizk, "Modeling of transmission line exposure to direct lightning strokes," *IEEE Trans. Power Del.*, vol. 5, no. 4, pp. 1983-1997, Oct. 1990.
- [20] N. I. Petrov, G. Petrova, and R. T. Waters, "Determination of attractive area and collection volume of earthed structures," in *Proc. 25th Int. Conf. Lightning Protection*, Rhodes, Greece, 2000, pp. 374-379.
- [21] A. Borghetti, C. A. Nucci, and M. Paolone, "Estimation of the statistical distributions of lightning current parameters at ground level from the data recorded by instrumented towers," *IEEE Trans. Power Del.*, vol. 19, no. 3, pp. 1400-1409, Jul. 2004.
- [22] L. Dellera and E. Garbagnati, "Lightning stroke simulation by means of the leader progression model," *IEEE Trans. Power Del.*, vol. 5, no. 4, pp. 2009-2029, Oct. 1990.
- [23] S. Ait-Amar and G. Berger, "A modified version of the rolling sphere method," *IEEE Trans. Dielectr. Electr. Insul.*, vol. 16, no. 3, pp. 718-725, Jun. 2009.
- [24] V. Cooray and M. Becerra, "Attractive radius and the volume of protection of vertical and horizontal conductors evaluated using a self consistent leader inception and propagation model – SLIM," in *Proc. 30th Int. Conf. Lightning Protection*, Cagliari, Italy, 2010, paper no. 1062.
- [25] P. N. Mikropoulos and T. E. Tsovilis, "Striking distance and interception probability," *IEEE Trans. Power Del.*, vol. 23, no. 3, pp. 1571-1580, Jul. 2008.
- [26] P. N. Mikropoulos and T. E. Tsovilis, "Interception probability and shielding against lightning," *IEEE Trans. Power Del.*, vol. 24, no. 2, pp. 863-873, Apr. 2009.
- [27] P. N. Mikropoulos and T. E. Tsovilis, "Interception probability and proximity effects: Implications in shielding design against lightning," *IEEE Trans. Power Del.*, vol. 25, no. 3, pp. 1940-1951, Jul. 2010.
- [28] P. N. Mikropoulos, T. E. Tsovilis, Z. G. Datsios, and N. C. Mavrikakis, "Effects of simulation models of overhead transmission line basic components on backflashover surges impinging on GIS substations," in *Proc. 45th UPEC*, Cardiff, Wales, 2010, paper no. 72.
- [29] M. A. Sargent and M. Darveniza, "Tower surge impedance," *IEEE Trans. Power App. Syst.*, vol. PAS-88, no. 5, pp. 680-687, May 1969.
- [30] A. Ametani and T. Kawamura, "A method of a lightning surge analysis recommended in Japan using EMTP," *IEEE Trans. Power Del.*, vol. 20, no. 2, pp. 867-875, Apr. 2005.
- [31] IEEE Task Force, "Modeling guidelines for fast front transients," *IEEE Trans. Power Del.*, vol. 11, no. 1, pp. 493-506, Jan. 1996.
- [32] P. Pinceti and M. Giannettini, "A simplified model for zinc oxide surge arresters," *IEEE Trans. Power Del.*, vol. 14, no. 2, pp. 393-398, Apr. 1999.
- [33] IEC 60071-2, *Insulation co-ordination – Part 2: Application guide*, 1996.
- [34] Joint Working Group 33/23.12, "Insulation co-ordination of GIS: Return of experience, on site tests and diagnostic techniques," *Electra*, no. 176, pp. 67-97, Feb. 1998.